HEMATOPOIESIS AND STEM CELLS

Ezh2 loss in hematopoietic stem cells predisposes mice to develop heterogeneous malignancies in an Ezh1-dependent manner

Makiko Mochizuki-Kashio,[1] Kazumasa Aoyama,[1] Goro Sashida,[1,2] Motohiko Oshima,[1] Takahisa Tomioka,[1,3] Tomoya Muto,[1] Changshan Wang,[1,4] and Atsushi Iwama[1]

[1]Department of Cellular and Molecular Medicine, Graduate School of Medicine, Chiba University, Chiba, Japan; [2]International Research Center for Medical Sciences, Kumamoto University, Kumamoto, Japan; [3]Department of Molecular Cell Biology, Graduate School of Pharmaceutical Sciences, Chiba University, Chiba, Japan; and [4]College of Life Sciences, Inner Mongolia University, Hohhot, China

Key Points

- Ezh2 loss in hematopoietic stem cells predisposes mice to develop heterogeneous hematologic malignancies.
- Ezh1 is essential to maintain hematopoiesis in the setting of Ezh2 loss.

Recent genome sequencing revealed inactivating mutations in *EZH2*, which encodes an enzymatic component of polycomb-repressive complex 2 (PRC2), in patients with myelodysplastic syndrome (MDS), myeloproliferative neoplasms (MPNs), and MDS/MPN overlap disorders. We herein demonstrated that the hematopoietic-specific deletion of *Ezh2* in mice induced heterogeneous hematopoietic malignancies. Myelodysplasia was detected in mice following the deletion of *Ezh2*, and resulted in the development of MDS and MDS/MPN. Thrombocytosis was induced by Ezh2 loss and sustained in some mice with myelodysplasia. Although less frequent, Ezh2 loss also induced T-cell acute lymphoblastic leukemia and the clonal expansion of B-1a B cells. Gene expression profiling showed that PRC2 target genes were derepressed upon the deletion of *Ezh2* in hematopoietic stem and progenitor cells, but were largely repressed during the development of MDS and MDS/MPN. Chromatin immunoprecipitation–sequence analysis of trimethylation of histone H3 at lysine 27 (H3K27me3) revealed a compensatory function of Ezh1, another enzymatic component of PRC2, in this process. The deletion of *Ezh1* alone did not cause dysplasia or any hematologic malignancies in mice, but abolished the repopulating capacity of hematopoietic stem cells when combined with Ezh2 loss. These results clearly demonstrated an essential role of Ezh1 in the pathogenesis of hematopoietic malignancies induced by *Ezh2* insufficiency, and highlighted the differential functions of Ezh1 and Ezh2 in hematopoiesis. (*Blood*. 2015;126(10):1172-1183)

Introduction

Polycomb-group (PcG) proteins function in the maintenance of gene silencing through histone modifications. They form several distinct polycomb-repressive complexes (PRCs), including canonical and non-canonical PRC1 and PRC2.[1,2] PRC2 consists of Eed, Suz12, and Ezh2 or its closely related homolog Ezh1. Ezh1 and Ezh2 are the catalytic components of PRC2 and catalyze the mono-, di-, and trimethylation of histone H3 at lysine 27 (H3K27me1/me2/me3). PcG proteins, including PRC2 components, have been characterized as general regulators of stem cells as well as tumorigenesis.[1,3,4] Eed and Ezh1, the core component of PRC2, were previously found to be essential for the maintenance of hematopoietic stem cells (HSCs).[5,6] Although Ezh2 is dispensable for the self-renewal capacity of adult bone marrow (BM) HSCs,[7] it is required to promote *MLL-AF9*–driven acute myeloid leukemia (AML) in mice,[8-10] and the forced expression of *Ezh2* in HSCs was shown to cause myeloproliferative neoplasms (MPNs) in mice.[11]

Comprehensive genome sequence studies initially identified activating mutations in *EZH2* in follicular and diffuse large B-cell lymphomas,[12] thereby supporting the oncogenic function of PRC2 in cancer. However, inactivating mutations in *EZH2* have also been identified in patients with myelodysplastic syndrome (MDS) (3%∼7%), MPNs (3%∼13%), and MDS/MPN overlap disorders (8%∼13%), which are all clonal myeloid disorders originating from HSCs.[13-20] Given that *EZH2*, which is located at chromosome 7q36.1, is frequently involved in chromosomal abnormalities such as −7 and 7q−, in hematologic malignancies,[21] these findings suggest a tumor suppressor role for EZH2 in these HSC disorders. Other components of PRC2, *EED* and *SUZ12*, are also targeted in somatic inactivating mutations, although the frequencies of their mutations were found to be markedly lower than those of *EZH2* mutations.[20] *ASXL1*, which plays an important role in the recruitment and/or stability of PRC2,[22] has also been shown to carry inactivating mutations in patients with MDS, MPN, and MDS/MPN.[20,23] Thus, the role of PRC2 in hematologic malignancies is complex.[19]

These findings prompted us to investigate the impact of inactivating *EZH2* mutations on hematopoiesis and its interplay with coinciding mutations such as *TET2* and *RUNX1* in mice. In our previous studies, the concurrent depletion of *Ezh2* and *Tet2* in mice markedly accelerated the development of MDS and MDS/MPN and Ezh2 loss significantly promoted *RUNX1S291fs*-induced MDS.[24,25] These findings support the tumor suppressor function of EZH2 in the context of myelodysplastic disorders. However, Ezh2 loss attenuated the predisposition of *RUNX1S291fs*-induced MDS cells to leukemic transformation,[25] which is consistent with the finding that inactivating mutations of *EZH2* are rare in de novo and secondary AML patients.[12,20,26,27] In our previous studies,

Submitted March 14, 2015; accepted July 21, 2015. Prepublished online as *Blood* First Edition paper, July 28, 2015; DOI 10.1182/blood-2015-03-634428.

The online version of this article contains a data supplement.

The publication costs of this article were defrayed in part by page charge payment. Therefore, and solely to indicate this fact, this article is hereby marked "advertisement" in accordance with 18 USC section 1734.

we also noted that the deletion of *Ezh2* alone induced myelodysplastic disorders after a long latency; however, detailed analysis was not performed.[24,25]

In contrast to *EZH2*, no somatic mutations have been identified in *EZH1* in hematologic malignancies.[20] As described above, conditional ablation of *Ezh1* in adult BM HSCs induces significant loss of adult HSCs, with concomitant impairment of their self-renewal capacity mainly due to derepression of *Cdkn2a*.[5] It is known that Ezh1 complements Ezh2 in maintaining pluripotency of $Ezh2^{-/-}$ embryonic stem cells (ESCs), and depletion of *Ezh1* abolishes residual methylation at H3K27 and derepresses H3K27me3 target genes, resulting in failure of the maintenance of ESC identity.[28] Given that *Ezh2*-deficient HSCs maintain self-renewal capacity,[7] Ezh1 may function as a critical backup enzyme also in the BM in the setting of Ezh2 loss.

In order to understand the pathological role of inactivating *EZH2* mutations in myeloid malignancies, we herein analyzed mice with the hematopoietic cell-specific deletion of *Ezh2* and determined how Ezh2 loss in HSCs predisposed mice to develop heterogeneous hematologic malignancies. We also examined the role of Ezh1 in the maintenance of hematopoiesis and in disease progression in the setting of Ezh2 loss.

Materials and methods

Mice

$Ezh2^{fl/fl}$ mice[29] were crossed with *Rosa26::Cre-ERT* mice (TaconicArtemis GmbH) to achieve the conditional deletion of *Ezh2*. These mice were injected with 100 μL of tamoxifen dissolved in corn oil at a concentration of 10 mg/mL intraperitoneally for 5 consecutive days to induce Cre-ERT activity. *Ezh1* constitutive knockout mice were obtained from Thomas Jenuwein's laboratory (Max Planck Institute of Immunobiology and Epigenetics, Freiburg, Germany) and will be reported elsewhere. Part of its phenotypes has been reported previously.[30,31] C57BL/6 mice congenic for the Ly5 locus (CD45.1) were purchased from Sankyo-Laboratory Service (Tsukuba, Japan). All animal experiments were performed in accordance with our institutional guidelines for the use of laboratory animals and approved by the Review Board for Animal Experiments of Chiba University (approval ID: 25-104).

Purification of hematopoietic cells

Mononuclear cells from BM were isolated on Ficoll-Paque PLUS (GE Healthcare) and incubated with a mixture of biotin-conjugated monoclonal antibodies (mAbs) against lineage markers including Gr-1, Mac-1, Ter-119, B220, interleukin-7Rα (IL-7Rα), CD4, and CD8α. The cells were further stained with allophycocyanin (APC)-Cy7–conjugated streptavidin and a combination of mAbs including phycoerythrin (PE)–Sca-1 and APC–c-Kit. The Pacific Blue–CD45.2 mAb was used as an additional marker for donor-derived cells.

BM transplantation

BM cells from CD45.2 mutant mice (test cells) were transplanted IV into 8- to 12-week-old CD45.1 recipients irradiated at a dose of 9.0 to 9.5 Gy with or without BM cells from 8- to 12-week-old CD45.1 congenic mice (competitor cells). The chimerism of donor-derived hematopoietic cells was monitored by flow cytometry. The proportion of donor cells was evaluated by dividing the number of CD45.2-single-positive cells by the total number of CD45-positive cells (CD45.1 + CD45.2).

Gene set enrichment analysis

We performed gene set enrichment analysis (GSEA) as described.[32] We excluded genes not detected in microarray analyses and those with no reads in both samples to be compared in RNA-sequence analyses from GSEA.

Statistical analysis

The statistical significance of differences was measured by the unpaired 2-tailed Student *t* test. When the variance was judged as significantly different by *f* test and the number of samples was enough ($n > 11$), we used the Mann-Whitney nonparametric test. These tests were carried out using Graph Pad Prism, version 6.

Results

Deletion of *Ezh2* caused myelodysplasia

To decipher the pathological role of inactivating *EZH2* mutations in hematologic malignancies, we transplanted BM cells from *Cre-ERT* control (wild-type [WT]) and *Cre-ERT;*$Ezh2^{fl/fl}$ CD45.2 mice (8-12 weeks old) without competitor cells into lethally irradiated CD45.1 recipient mice and deleted *Ezh2* by intraperitoneal injection of tamoxifen at 6 to 8 weeks posttransplantation (supplemental Figure 1A, available on the *Blood* Web site). We confirmed the efficient deletion of *Ezh2* in hematopoietic cells from $Ezh2^{\Delta/\Delta}$ mice by genomic polymerase chain reaction (PCR) (supplemental Figure 2). We hereafter referred to the recipient mice reconstituted with WT and $Ezh2^{\Delta/\Delta}$ cells as WT and $Ezh2^{\Delta/\Delta}$ mice, respectively.

As we reported previously,[7] chimerism of the lymphoid lineage, particularly of the B lymphoid lineage, was significantly reduced in the peripheral blood (PB) whereas that of the myeloid lineage was increased over time after the deletion of *Ezh2* (supplemental Figure 1C). Correspondingly, the white blood cell count in the PB was significantly decreased in $Ezh2^{\Delta/\Delta}$ mice, whereas the platelet count significantly increased (supplemental Figure 1B). Anemia was also more severe in $Ezh2^{\Delta/\Delta}$ mice than in control mice (supplemental Figure 1B). However, BM analysis 3 months after the deletion of *Ezh2* did not detect any significant changes in the BM cell counts and the numbers of $CD34^-$ LSK HSCs and LSK hematopoietic stem and progenitor cells (HSPCs) (supplemental Figure 1D). The proportion of Annexin V^+ cells in $CD71^+Ter119^+$ erythroblasts was mildly increased in $Ezh2^{\Delta/\Delta}$ mice compared with WT mice, albeit not statistically significant, implicating enhanced inefficient hematopoiesis in the BM, a feature compatible with myelodysplastic disorders (supplemental Figure 1E). Morphologic dysplasia, which is characteristic of myelodysplastic disorders, became gradually evident in the PB of $Ezh2^{\Delta/\Delta}$ mice over time, including pseudo-Pelger-Huët cells, hypersegmented neutrophils, Howell-Jolly bodies, and giant platelets (supplemental Figure 1F). These findings indicate that deletion of *Ezh2* caused myelodysplasia in mice.

$Ezh2^{\Delta/\Delta}$ mice developed myelodysplastic disorders

Although no significant difference was observed in the survival of $Ezh2^{\Delta/\Delta}$ mice by 10 months after the deletion of *Ezh2* (Figure 1A), they developed myelodysplastic disorders during a long observation period (Figure 1B; supplemental Table 1). We previously reported the development of MDS/MPN, but not MDS in $Ezh2^{\Delta/\Delta}$ mice.[24] However, $Ezh2^{\Delta/\Delta}$ mice in the present study developed both MDS/MPN and MDS (Figure 1B). All $Ezh2^{\Delta/\Delta}$ mice showed morphologic dysplasia of hematopoietic cells as presented above (supplemental Figure 1F; supplemental Table 1). MDS/MPN mice exhibited myeloproliferative features, including splenomegaly with active extramedullary hematopoiesis, an increase in the number of LSK cells in the BM and/or the spleen, and chronic myelomonocytic leukemia (CMML)-like monocytosis in the PB. In contrast, MDS mice did not display

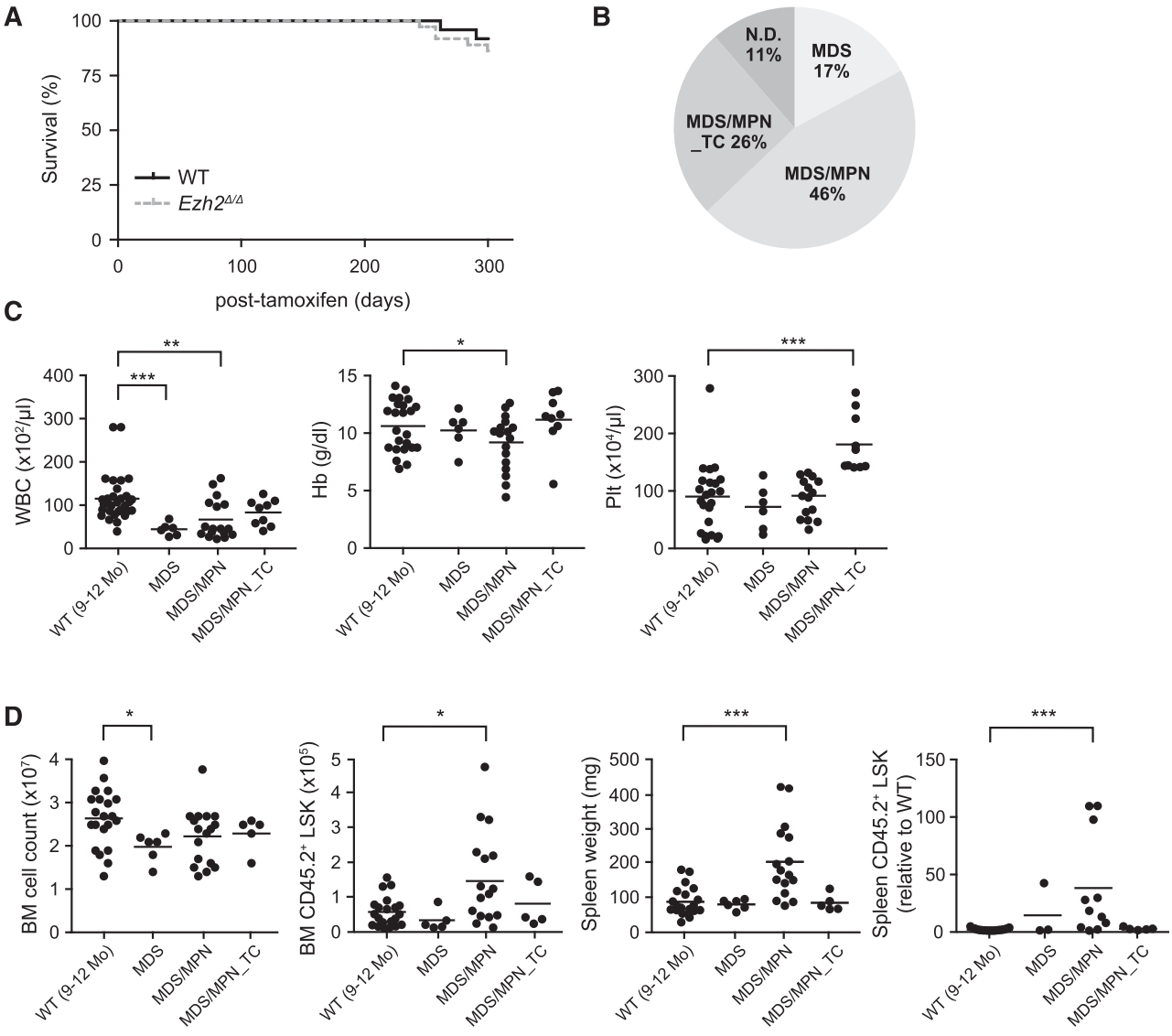

Figure 1. *Ezh2*$^{\Delta/\Delta}$ mice developed myelodysplastic disorders. (A) Kaplan-Meier survival curves of WT (n = 24) and *Ezh2*$^{\Delta/\Delta}$ (n = 32) mice. These survival curves were generated from 3 independent experiments. (B) A pie graph showing the types of hematologic malignancies observed in *Ezh2*$^{\Delta/\Delta}$ mice (n = 32) during a long observation period. (C) PB cell counts in *Ezh2*$^{\Delta/\Delta}$ mice 9 to 12 months after the deletion of *Ezh2*. WBC, Hb, and Plt counts in the PB from WT (n = 24) and *Ezh2*$^{\Delta/\Delta}$ MDS (n = 6), MDS/MPN (n = 17), and MDS/MPN_TC (n = 9) mice are plotted as dots and the mean values are indicated as bars. (D) Absolute numbers of total BM cells and LSK cells in a unilateral femur, and spleen weights and numbers of LSK cells in the spleen relative to WT are plotted as dots and mean values are indicated as bars (WT, n = 21; MDS, n = 6; MDS/MPN, n = 16; MDS/MPN_TC, n = 5). Statistical significance of difference was measured by unpaired 2-tailed Student *t* test or Mann-Whitney test when the variance was judged as significantly different by *f* test. *$P < .05$, **$P < .01$, ***$P < .001$. Hb, hemoglobin; ND, not determined; Plt, platelet; WBC, white blood cell.

any obvious myeloproliferative features, but were more likely to develop cytopenia (Figure 1C-D; supplemental Table 1). Some *Ezh2*$^{\Delta/\Delta}$ mice developed MDS/MPN that was characterized by a significant increase in platelet numbers and mild myeloproliferative features in the BM and spleen (Figure 1C-D; supplemental Table 1). We categorized these mice as MDS/MPN with thrombocytosis (MDS/MPN_TC). Thus, *Ezh2*$^{\Delta/\Delta}$ mice developed myelodysplastic disorders including MDS, MDS/MPN, and MDS/MPN_TC.

Serial transplantation of *Ezh2*$^{\Delta/\Delta}$ hematopoietic cells caused heterogeneous hematologic malignancies

To clarify whether the myelodysplastic disorders induced by Ezh2 loss were transplantable, we transplanted BM cells from MDS and MDS/MPN mice ~10 months after the deletion of *Ezh2* into secondary recipients (Figure 2A). In contrast to the primary transplantation, *Ezh2*$^{\Delta/\Delta}$ mice developed hematologic malignancies markedly earlier after secondary transplantation (Figure 2B; supplemental Table 2). Four recipient mice, which developed T-cell acute lymphoblastic leukemia (ALL) of a CD45.1$^+$ host cell origin, were excluded from the present study (supplemental Table 2). *Ezh2*$^{\Delta/\Delta}$ mice developed more diverse diseases, including MDS, T-ALL/lymphoma, and lymphoproliferative disease (LPD) of B-1a B cells (Figure 2C-D; supplemental Table 2).

Four mice developed T-ALL/lymphoma with the prominent expansion of CD8α^+Tcr$\alpha\beta^+$ T cells in the thymus (Figure 2E). They also showed variable levels of infiltration of tumor cells in the PB (Figure 2D-E) and other organs (data not shown). To understand the molecular basis of *Ezh2*$^{\Delta/\Delta}$ T-ALL, we performed RNA-sequence

A

Donor no.	Diagnosis	Cell count	Irradiation	Engraftment
1	MDS/MPN	2.5x10^6	sublethal	4/4
2	CMMoL	2.5x10^6	sublethal	4/4
3	MDS/MPN	2.5x10^6	sublethal	4/4
4	MDS	2.5x10^6	lethal	4/4
5	WT	2.5x10^6	sublethal	4/4

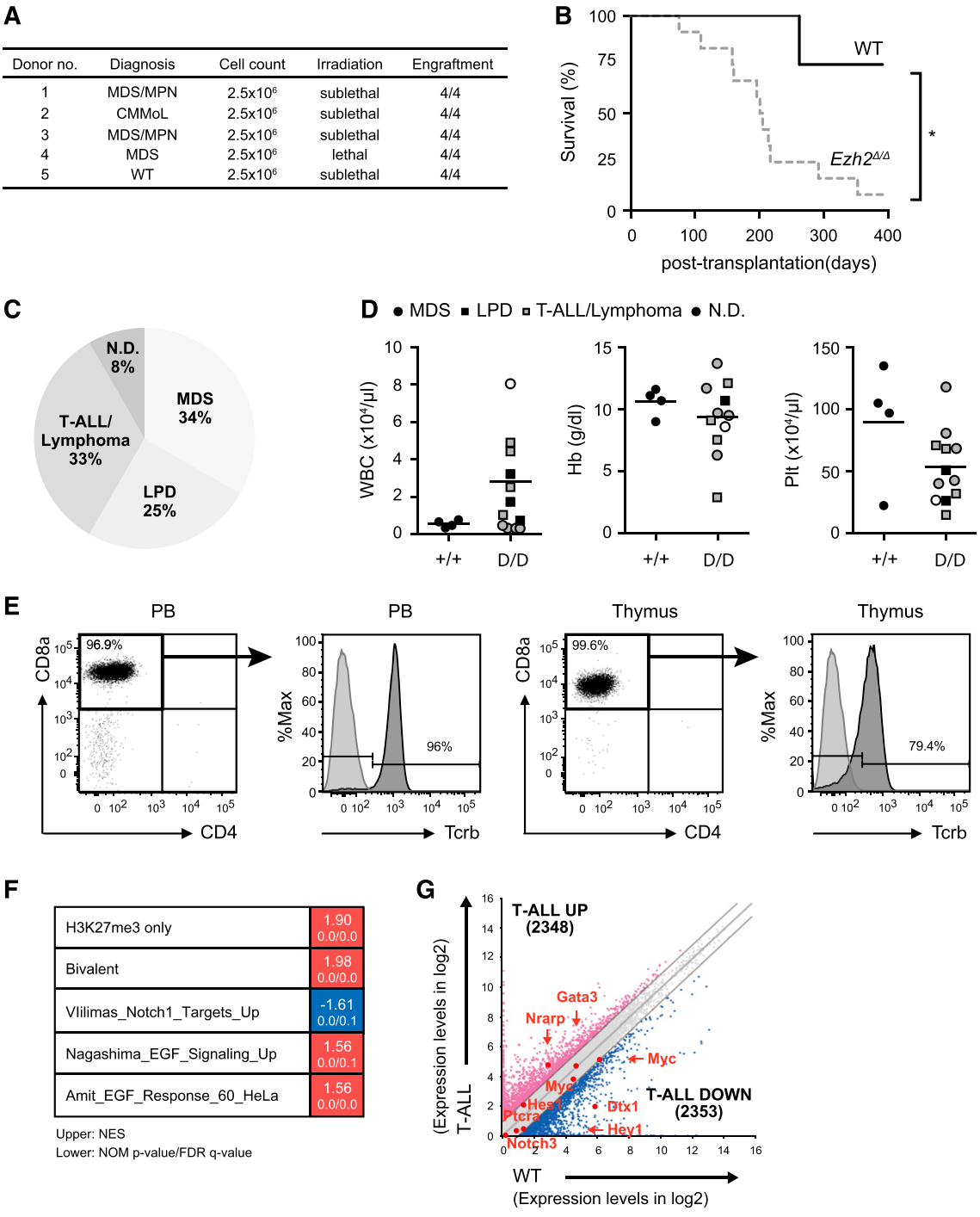

Figure 2. Serial transplantation of *Ezh2*$^{\Delta/\Delta}$ hematopoietic cells caused heterogeneous hematologic malignancies. (A) Summary of secondary transplantation. A total of 2.5 × 10^6 BM cells from MDS and MDS/MPN mice ~10 months after the deletion of *Ezh2* were transplanted into secondary recipients irradiated at a lethal (8.5 Gy) or sublethal (6.5 Gy) dose. The engraftment status is indicated. (B) A Kaplan-Meier survival curve of WT (n = 4) and *Ezh2*$^{\Delta/\Delta}$ (n = 12) mice in secondary transplantation. Four recipient mice, which developed CD45.1$^+$ T-ALL of a host cell origin, were excluded. *$P < .05$. Statistical significance was measured by log-rank test. (C) A pie graph showing the types of hematologic malignancies observed in *Ezh2*$^{\Delta/\Delta}$ mice (n = 12) in the secondary transplantation. Four recipient mice, which developed CD45.1$^+$ T-ALL of a host cell origin, were excluded. (D) PB cell counts of moribund mice and those surviving at 370 days after secondary transplantation. WBC, Hb, and Plt counts in the PB of *Ezh2*$^{\Delta/\Delta}$ MDS, LPD, and T-ALL/lymphoma mice are plotted as dots and the mean values are indicated as bars. (E) Flow cytometric profiles of donor-derived CD45.2$^+$ T-ALL/lymphoma cells in the PB and thymus obtained from representative mice with T-ALL/lymphoma (11F8_004, supplemental Table 2) at 52 weeks posttransplantation. Unstained cells served as a control for Tcrβ staining. (F) Gene expression profiling of *Ezh2*$^{\Delta/\Delta}$ T-ALL cells. RNA sequence was performed using *Ezh2*$^{\Delta/\Delta}$ BM CD8$^+$ T-ALL cells obtained from a *Ezh2*$^{\Delta/\Delta}$ mouse with T-ALL and WT BM CD8$^+$ T cells. GSEA was performed using the RNA-sequence data and GSEA plots are shown. The NES, NOM *P* value, and FDR q value are indicated. (G) Scatter diagrams showing RNA-sequence data. The signal levels of RefSeq genes (RPKM + 1 in log2) in *Ezh2*$^{\Delta/\Delta}$ BM CD8$^+$ T-ALL cells and WT BM CD8$^+$ T cells are plotted. The light gray lines represent the boundaries for twofold increase and twofold decrease, respectively. The number of genes upregulated and downregulated more than twofold in *Ezh2*$^{\Delta/\Delta}$ T-ALL cells compared with WT cells are indicated. The representative direct target genes of Notch1 are shown as red dots. FDR, false discovery rate; NES, normalized enrichment score; NOM, nominal.

analysis of BM $CD8^+$ T-ALL cells and WT BM $CD8^+$ T cells. GSEA revealed positive enrichment of PRC2 targets defined in HSCs, including those marked with H3K27me3 alone (H3K27me3 only) as well as those with H3K27me3 and H3K4me3 (bivalent genes) at their promoters (Figure 2F; supplemental Table 3).[33] It has been reported that 25% of T-ALL patients have loss-of-function mutations in the PRC2 gene, mostly in *EZH2*, and 65% of the patients with PRC2 gene mutations concurrently have activating *NOTCH1* mutations.[34] These findings suggest that *EZH2* and *NOTCH1* mutations directly or indirectly cooperate in T-ALL. In $Ezh2^{\Delta/\Delta}$ T-ALL, however, direct targets of Notch1 were not significantly activated (Figure 2G) and the Notch target gene set was negatively enriched (Figure 2F), suggesting that T-ALL that developed in the absence of Ezh2 in mice required activation of additional pathways other than Notch. In this regard, positive enrichment of the epidermal growth factor signaling gene sets is intriguing (Figure 2F), but requires extensive validation.

Most $Ezh2^{\Delta/\Delta}$ mice had $CD19^+B220^{mid}CD5^+IgM^+$ B-1a B cells in the PB at variable levels (supplemental Figure 3A-B). Among these, some mice developed lymphoproliferative neoplasm of B-1a B cells. Although we did not precisely examine B-1a B cell expansion in primary recipients, we observed the expansion of $B220^{low}$ non-T ($CD4^-CD8^-$), nonmyeloid cells in the PB of 16 of 36 mice, which were thought to be B-1a B cells (supplemental Table 1). Most of the B-1a B cells were polyclonal by genomic PCR of the D-J rearrangement of the *Igh* gene. However, some mice showed clonal expansion, and were, thus, assumed to have developed into chronic lymphocytic leukemia (CLL) (supplemental Figure 3C; supplemental Tables 1-2). These results indicated that Ezh2 loss predisposed mice to heterogeneous hematologic malignancies.

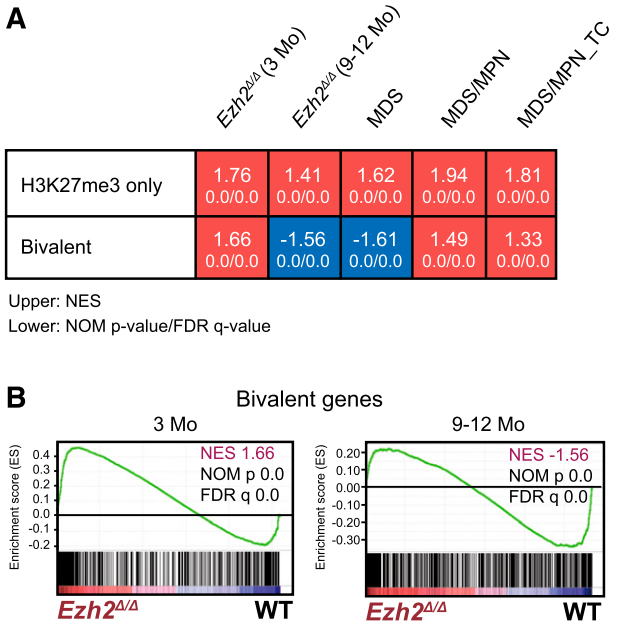

Figure 3. Loss of Ezh2 reprogrammed the transcriptional landscape of HSPCs. (A) Gene expression alterations associated with disease progression. GSEA was performed using the microarray analysis data of WT and $Ezh2^{\Delta/\Delta}$ LSK cells from early and late time points after the deletion of *Ezh2* (3 and 9-12 months, respectively). LSK cells were also collected individually from MDS (10F14 and 11F2), MDS/MPN (11F5), and MDS/MPN_TC mice (10F7) ~10 months after the deletion of *Ezh2*. The NES from the gene expression profiles of LSK cells derived from GSEA is shown as a number in each cell. The NOM *P* value and FDR are shown below NES. Red and blue colors represent positive (upregulated in the given genotype relative to WT) and negative (upregulated in WT relative to the given genotype) enrichment, respectively. (B) Gene set enrichment plots for the bivalent gene set in HSCs in panel A comparing $Ezh2^{\Delta/\Delta}$ LSK cells to WT LSK cells 3 and 9 to 12 months after the deletion of *Ezh2*.

Loss of Ezh2 reprogrammed the transcriptional landscape of HSPCs

In order to understand the molecular mechanism underlying myelodysplastic disorders induced by *Ezh2* insufficiency in more detail, we performed gene expression profiling by a microarray analysis using LSK cells collected from 3 to 5 mice randomly selected at early and late time points after the deletion of *Ezh2* (3 and 9-12 months, respectively). LSK cells were also collected individually from MDS (n = 2), MDS/MPN (n = 1), and MDS/MPN_TC (n = 1) mice ~9 to 12 months after the deletion of *Ezh2*.

We performed a GSEA. As expected, PRC2 targets defined in HSCs, including H3K27me3-only genes (marked only with H3K27me3) and bivalent genes (marked with H3K27me3 and H3K4me3) (supplemental Table 3),[33] were again more likely to be derepressed and were more positively enriched in LSK cells 3 months after the deletion of *Ezh2* than in WT LSK cells (Figure 3). Of note, only bivalent genes became negatively enriched with significance in LSK cells at later time points (9-12 months after the deletion of *Ezh2*) and in MDS LSK cells, whereas H3K27me3-only genes remained positively enriched. These results suggest that Ezh1, the only H3K27 methyltransferase in the absence of Ezh2, becomes functionally augmented in myelodysplastic disorders and largely complements Ezh2 loss, particularly at the promoters of bivalent genes.

Western blot analysis, however, did not show any significant changes in global H3K27me3 levels between the early (1 month) and late (9 months) time points postdeletion of *Ezh2* (supplemental Figure 4). Thus, we next performed chromatin immunoprecipitation (ChIP)-sequence analysis of H3K27me3. As evident in scatter plots of H3K27me3 signals, H3K27me3 levels at promoters significantly increased in LSK cells at 9 months compared with 1 month postdeletion of *Ezh2* (Figure 4A). We then categorized genes with ChIP signals >1 against the input signals depending on the changes in H3K27me3 levels at 1 and 9 months postdeletion of *Ezh2*. We defined genes that lost H3K27me3 levels at least twofold at 1-month postdeletion of *Ezh2* as "Ezh2 target genes." Among these, 3605 genes that gained H3K27me3 levels at least twofold at 9 months compared with 1 month postdeletion of *Ezh2* were defined as "Ezh2 targets with Ezh1 compensation (Ezh2 target/Ezh1 Comp)." In contrast, 969 genes that did not gain H3K27me3 levels were defined as "Ezh2 targets with no Ezh1 compensation (Ezh2 target/Ezh1 no Comp)." We also defined 1966 genes that did not lose H3K27me3 levels at least twofold at 1-month postdeletion of *Ezh2* and did not show any significant changes thereafter as "Ezh1 target genes" (Figure 4B; supplemental Table 3). ChIP-sequence data of the representative gene loci of each category are visualized in Figure 4C. Of note, only Ezh2 target/Ezh1 Comp genes showed moderate but significant trend toward gene repression at 9 to 12 months compared with 3 months postdeletion of *Ezh2* (Figure 4D).

Bivalent genes appeared to largely overlap with Ezh2 target/Ezh1 Comp genes (Figure 4E), thus showing an increase in the H3K27me3 levels at 9 months compared with 1 month postdeletion of *Ezh2* (Figure 4F) and a moderate but significant trend toward gene repression over time (Figure 4G). In contrast, the expression profile of H3K27-only genes did not change over time (Figure 4G) as demonstrated in GSEA (Figure 3A). These findings indicate that the recovery of H3K27me3 levels takes place not globally but in a locus-specific manner over time and suggest repositioning of Ezh1 to Ezh2 targets to complement Ezh2 loss.

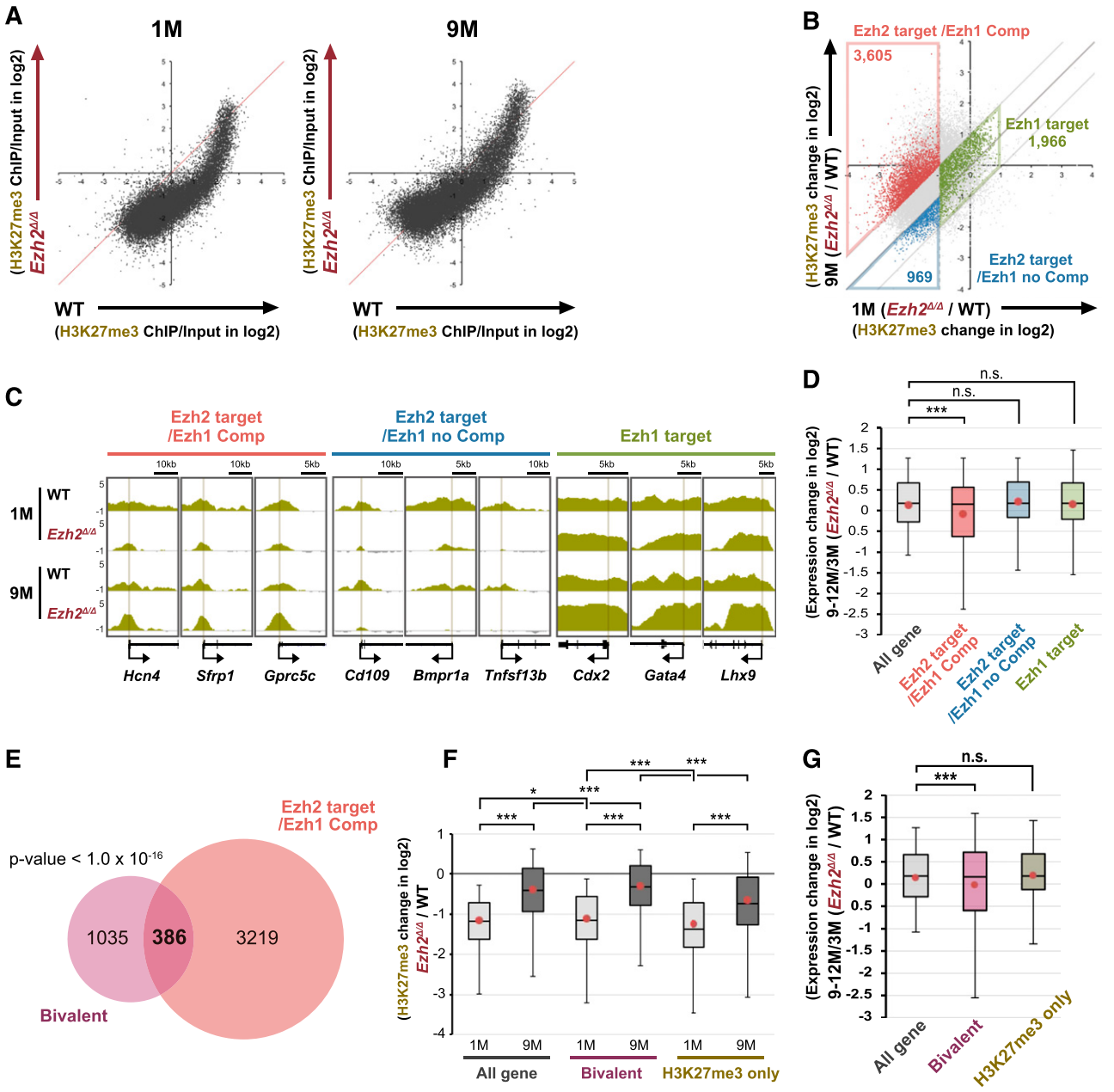

Figure 4. Restoration of H3K27me3 levels at part of Ezh2 target gene promoters in *Ezh2*$^{\Delta/\Delta}$ HSPCs. (A) Scatter plots showing the correlation of the fold enrichment values (ChIP/input) (transcription start site ± 2.0 kb) of H3K27me3 against the input signals of RefSeq genes between WT and *Ezh2*$^{\Delta/\Delta}$ LSK cells from WT and *Ezh2*$^{\Delta/\Delta}$ mice at 1 and 9 months postdeletion of *Ezh2*. (B) A scatter plot showing the correlation of H3K27me3 levels in *Ezh2*$^{\Delta/\Delta}$ LSK cells against WT LSK cells (*Ezh2*$^{\Delta/\Delta}$/WT) between 1 and 9 months postdeletion of *Ezh2*. The diagonal light gray lines represent the boundaries for twofold increase and twofold decrease, respectively. The vertical line represents the boundary for twofold reduction in fold enrichment of H3K27me3 in *Ezh2*$^{\Delta/\Delta}$ LSK cells at 1 month postdeletion of *Ezh2*. The genes with ChIP signals >1 over the input signals were categorized depending on the changes in H3K27me3 levels at 1 and 9 months postdeletion of *Ezh2*. The genes that lost H3K27me3 levels at least twofold at 1 month postdeletion of *Ezh2* were defined as "Ezh2 targets." Among these, the genes that gained H3K27me3 levels at least twofold at 9 months compared with 1 month postdeletion of *Ezh2* were defined as "Ezh2 target/Ezh1 Comp." In contrast, the genes that did not gain H3K27me3 levels were defined as "Ezh2 target/Ezh1 no Comp." The genes that did not lose H3K27me3 levels twofold at 1 month postdeletion of *Ezh2* and did not show any significant changes thereafter were defined as "Ezh1 target genes." Each category was boxed. (C) Visualization of ChIP-sequence data of H3K27me3 levels of representative genes that belong to the indicated categories defined in panel A in WT and *Ezh2*$^{\Delta/\Delta}$ LSK cells at 1 and 9 months postdeletion of *Ezh2* using the Integrative Genomics Viewer (IGV). Schematic diagrams of these gene loci indicate their genomic structures. Exons and untranslated regions are demarcated by large and small black boxes, respectively. (D) Box-and-whisker plots showing the expression changes of indicated genes in *Ezh2*$^{\Delta/\Delta}$ LSK cells relative to WT LSK cells (*Ezh2*$^{\Delta/\Delta}$/WT) at 9 to 12 months compared with 3 months postdeletion of *Ezh2*. Boxes represent 25 to 75 percentile ranges. Vertical lines represent 10 to 90 percentile ranges. Horizontal bars represent median. Mean values are indicated by red dots. Microarray data in Figure 3 were applied to this analysis. ***$P < .001$ (Student *t* test). (E) Venn diagram showing the overlap between Ezh2 target/Ezh1 Comp genes in panel B and bivalent genes. $P < 1.0 \times 10^{-16}$. (F) Box-and-whisker plots showing the changes in H3K27me3 levels of indicated genes in *Ezh2*$^{\Delta/\Delta}$ LSK cells relative to WT LSK cells (*Ezh2*$^{\Delta/\Delta}$/WT) at 1 and 9 months postdeletion of *Ezh2*. Mean values are indicated by red dots. *$P < .05$, ***$P < .001$ (Student *t* test). (G) Box-and-whisker plots showing the expression changes of indicated genes in *Ezh2*$^{\Delta/\Delta}$ LSK cells relative to WT LSK cells (*Ezh2*$^{\Delta/\Delta}$/WT) at 9 to 12 months compared with 3 months postdeletion of *Ezh2*. Mean values are indicated by red dots. Microarray data in Figure 3 was applied to this analysis. ***$P < .001$ (Student *t* test). ns, not significant.

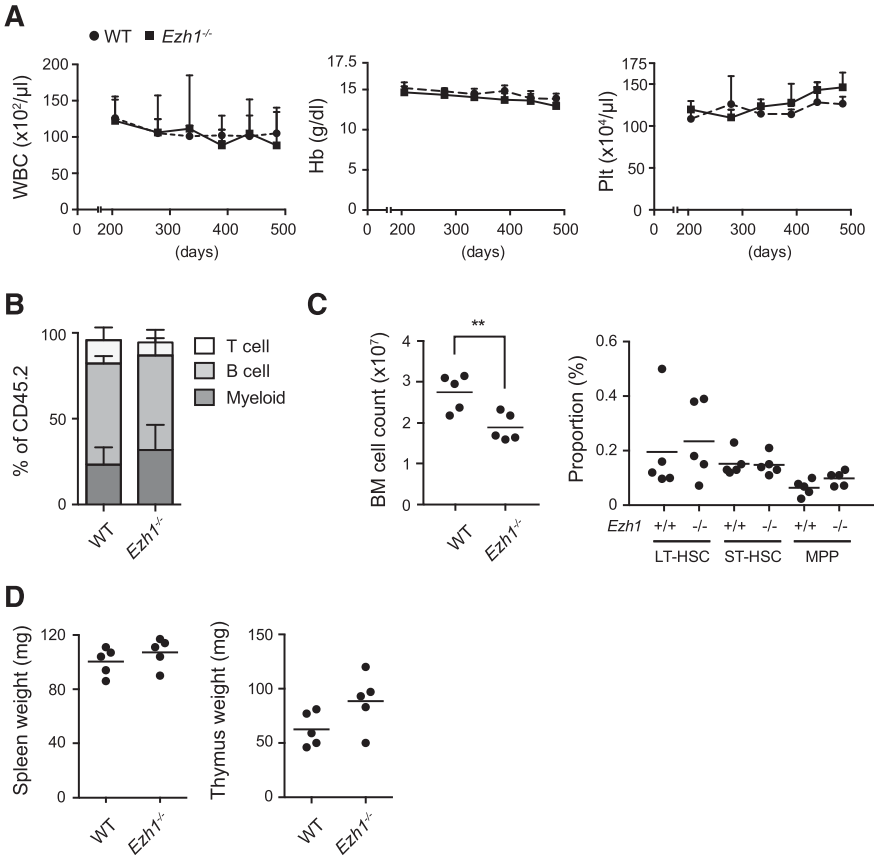

Figure 5. Ezh1 loss did not cause any hematologic malignancies. (A) PB cell counts in $Ezh1^{-/-}$ mice up to 16.5 months after birth. WBC, Hb, and Plt counts in the PB from WT (n = 5) and $Ezh1^{-/-}$ (n = 5) mice are shown as the mean ± standard deviation (SD). (B) The proportions of myeloid (Mac-1$^+$), B220$^+$ B, and CD4$^+$ or CD8$^+$ T cells among CD45$^+$ donor-derived hematopoietic cells in the PB at the time points indicated. Data are shown as the mean ± SD (n = 5). (C) Absolute numbers of total BM cells (left panel) and long-term (LT), short-term (ST), and multipotent progenitors (MPPs) in a unilateral pair of the femur and tibia from $Ezh1^{-/-}$ mice 16.5 months after birth. Data are plotted as dots and the mean values are indicated as bars (WT, n = 5; $Ezh1^{-/-}$, n = 5). (D) Weights of the spleen and thymus from $Ezh1^{-/-}$ mice 16.5 months after birth. Data are plotted as dots and the mean values are indicated as bars (WT, n = 5; $Ezh1^{-/-}$, n = 5). Statistical significance of difference was measured by unpaired 2-tailed Student *t* test. $^{**}P < .005$.

Ezh1 was essential for the maintenance of *Ezh2* insufficient myelodysplastic disorders

As we have previously reported[7,24] and also supported in this study, Ezh1 may play a critical role in the maintenance of hematopoiesis and also in disease progression in the absence of Ezh2. To address this issue, we analyzed *Ezh1* constitutive knockout mice.[30,31] Mice lacking *Ezh1* are viable, fertile, and healthy, and lack *Ezh1* mRNA.[31] We observed $Ezh1^{-/-}$ mice up to 16.5 months. They showed no hematologic abnormalities in the PB including cell blood counts (Figure 5A), lineage composition (Figure 5B), and cell morphology (data not shown). Although total BM cell numbers were significantly reduced, the absolute number of HSCs and progenitors in the BM was similar to that in the WT control (Figure 5C). The sizes of the thymus and spleen were also similar to those of the WT control (Figure 5D). These results clearly indicated that *Ezh1* insufficiency alone did not cause hematologic malignancies. This finding corresponds well to the finding that no inactivating mutations in *EZH1* have been identified in hematologic malignancies in contrast to *EZH2*.

To directly validate the role of Ezh1 in hematopoiesis in the absence of Ezh2, we then generated *Cre-ERT;*$Ezh1^{-/-}Ezh2^{fl/fl}$ mice (CD45.2), transplanted BM cells into lethally irradiated recipient mice, and then deleted *Ezh2* by injecting tamoxifen at 6 weeks posttransplantation. The deletion of *Ezh2* induced cytopenia in the PB of $Ezh1^{-/-}Ezh2^{\Delta/\Delta}$ mice, and $Ezh1^{-/-}Ezh2^{\Delta/\Delta}$ cells, particularly myeloid cells, were progressively depleted. Instead, residual CD45.1$^+$ host cells gradually overtook $Ezh1^{-/-}Ezh2^{\Delta/\Delta}$ cells and largely restored the blood cell counts in the PB. (Figure 6A). We subsequently evaluated the capacity of $Ezh1^{-/-}Ezh2^{\Delta/\Delta}$ HSCs to repopulate hematopoiesis by competitive repopulating assays. We transplanted *Cre-ERT;*$Ezh1^{-/-}Ezh2^{fl/fl}$ BM cells along with twice more BM competitor cells into lethally irradiated recipients. At 6 weeks posttransplantation, *Ezh2* was deleted by injecting tamoxifen. $Ezh1^{-/-}Ezh2^{\Delta/\Delta}$ donor cells were rapidly outcompeted by the competitor cells and the donor cells were depleted from both the PB and BM (Figure 6B-C).

In order to understand the molecular mechanism underlying the impaired repopulating capacity of $Ezh1^{-/-}Ezh2^{f\Delta/\Delta}$ HSCs in more detail, we examined the canonical polycomb targets, $p15^{Ink4b}$, $p16^{Ink4a}$, and $p19^{Arf}$, which are critical for the maintenance of HSC activity.[3,4,35,36] As expected, all of these tumor suppressor genes were markedly upregulated in $Ezh1^{-/-}Ezh2^{\Delta/\Delta}$ LSK and Lin$^-$c-Kit$^+$ cells (Figure 6D), but not in $Ezh1^{-/-}$ and $Ezh2^{\Delta/\Delta}$ cells (Figure 6D; supplemental Figure 5).

To check how Ezh1 can complement Ezh2 loss in hematopoiesis, we next performed RNA-sequence analysis of $Ezh1^{-/-}$ and $Ezh2^{\Delta/\Delta}$ LSK cells from recipient mice at 1-month postinjection of tamoxifen. Regardless of their modest hematologic phenotypes, $Ezh1^{-/-}$ LSK cells showed changes in gene expression profiles similar to $Ezh2^{\Delta/\Delta}$ LSK cells and a significant part of genes altered in $Ezh1^{-/-}$ and $Ezh2^{\Delta/\Delta}$ LSK cells overlapped (Figure 7A). GSEA revealed that Ezh1 loss also caused derepression of PRC2 target genes including H3K27me3-only genes and bivalent genes (Figures 7B), although the derepression levels were milder than those noticed with Ezh2 loss (Figure 7C). These findings indicate that the targets of Ezh1 and Ezh2 largely overlap. Of interest, the HSC gene signature defined by Chambers et al[37] was positively and negatively enriched in $Ezh2^{\Delta/\Delta}$ and $Ezh1^{-/-}$ LSK cells, respectively, although statistically not significant (Figure 7B). This finding may partly account for a tumor suppressor function of Ezh2 but not Ezh1 in myelodysplastic disorders. RNA-sequence data revealed no significant change in Ezh1 mRNA levels in $Ezh2^{\Delta/\Delta}$ LSK cells (Figure 7D).

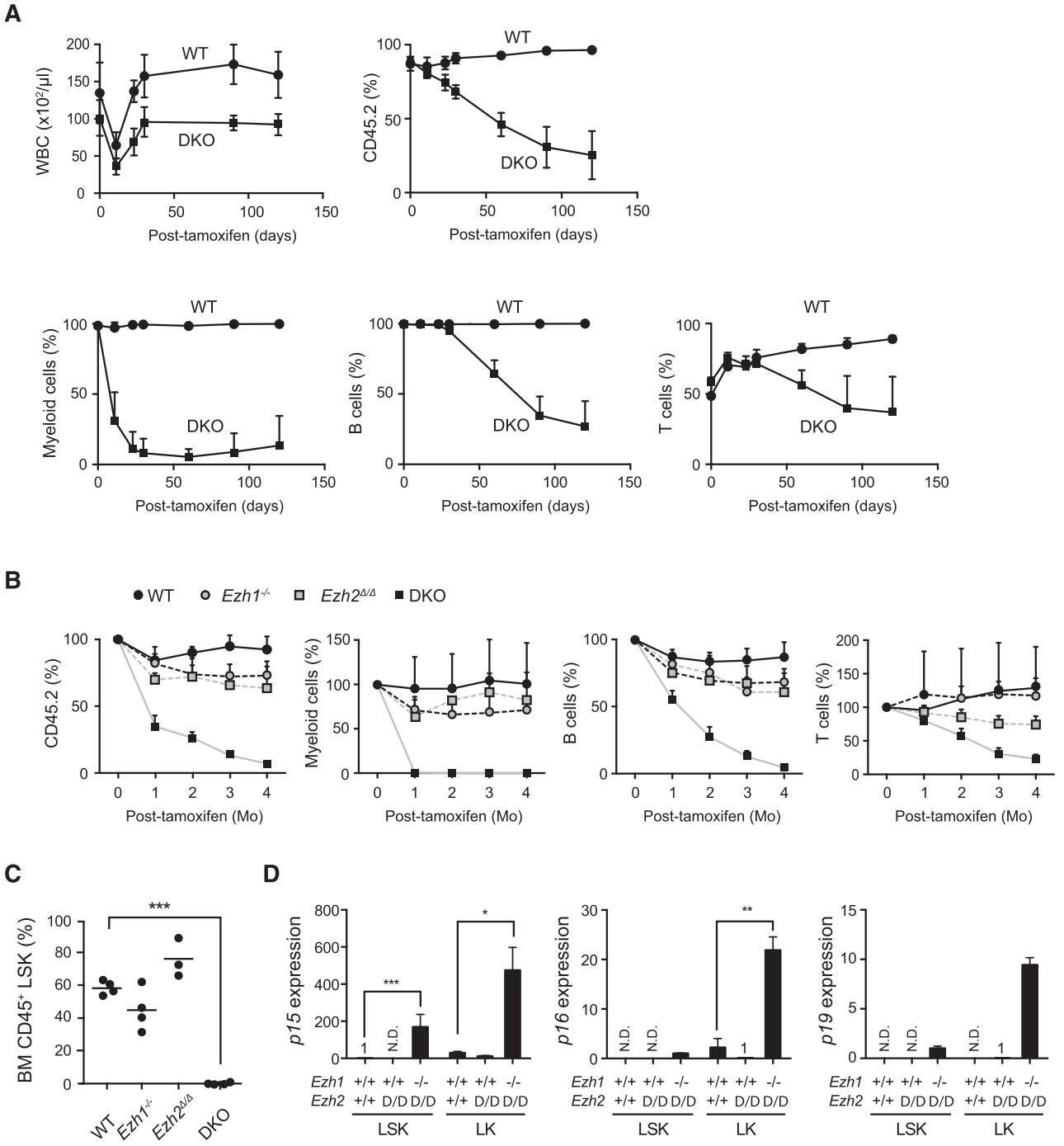

Figure 6. Ezh1 was essential for the maintenance of *Ezh2* insufficient hematopoiesis. (A) The failure of *Ezh1*$^{-/-}$*Ezh2*$^{\Delta/\Delta}$ hematopoietic cells to maintain hematopoiesis. BM cells from *Cre-ERT* and *Cre-ERT;Ezh1*$^{-/-}$*Ezh2*$^{fl/fl}$ mice were transplanted into lethally irradiated recipient mice without rescue BM cells, and *Ezh2* was then deleted by injecting tamoxifen at 6 weeks posttransplantation. Following tamoxifen injection, the recipient mice were fed with a tamoxifen diet (400 mg of tamoxifen citrate per kg diet) for 10 days. WBC counts, the chimerism of CD45.2$^+$ donor-derived cells, including Mac-1$^+$ myeloid cells, B220$^+$ B cells, and CD4$^+$ or CD8$^+$ T cells, in the PB from WT (n = 5) and *Ezh1*$^{-/-}$*Ezh2*$^{\Delta zh}$ (double knockout [DKO]) mice (n = 5) are shown as the mean ± SD. (B-C) Competitive repopulating assays. BM cells (CD45.2) from *Cre-ERT*, *Ezh1*$^{-/-}$, *Cre-ERT;Ezh2*$^{fl/fl}$, and *Cre-ERT;Ezh1*$^{-/-}$*Ezh2*$^{fl/fl}$ mice were transplanted into lethally irradiated recipient mice (CD45.1) with twice more competitor BM cells (CD45.1), and *Ezh2* was then deleted by injecting tamoxifen at 8 weeks posttransplantation. The chimerism of donor-derived CD45.2$^+$ cells, Mac-1$^+$ myeloid cells, B220$^+$ B cells, and CD4$^+$ or CD8$^+$ T cells in the PB is shown as percentage of chimerism values prior to the treatment with tamoxifen in panel B. Donor chimerism in BM LSK cells at 12 weeks posttransplantation is shown in panel C. Data are plotted as dots and the mean values are indicated as bars (n = 3-4, each). (D) A quantitative reverse transcription PCR (RT-PCR) analysis of CDK inhibitors (*p15*^{Ink4b}, *p16*^{Ink4a} and *p19*^{Arf}) in WT, *Ezh2*$^{\Delta/\Delta}$, and *Ezh1*$^{-/-}$*Ezh2*$^{\Delta/\Delta}$ LSK and LK cells 2 weeks after the deletion of *Ezh2*. mRNA levels were normalized to *Hprt1* expression and relative expression levels are shown as the mean ± SD for triplicate analyses. The cells whose expression was arbitrarily set to 1 are indicated as "1". Statistical significance of difference was measured by unpaired 2-tailed Student *t* test. **P* < .05, ***P* < .01, ****P* < .001.

Finally, we checked the expression of *EZH1* and *EZH2* in human MDS patients.[38] As expected, *EZH2* expression was significantly downregulated in CD34$^+$ cells from MDS patients and this trend was more significant in CD34$^+$ cells from MDS patients with the 7q deletion, which often results in the loss of *EZH2* at 7q36.1 (Figure 7E). In contrast, *EZH1* expression was comparable between controls and MDS patients. These findings indicate that the compensatory function of EZH1 in the setting of EZH2 loss is not regulated by its expression,

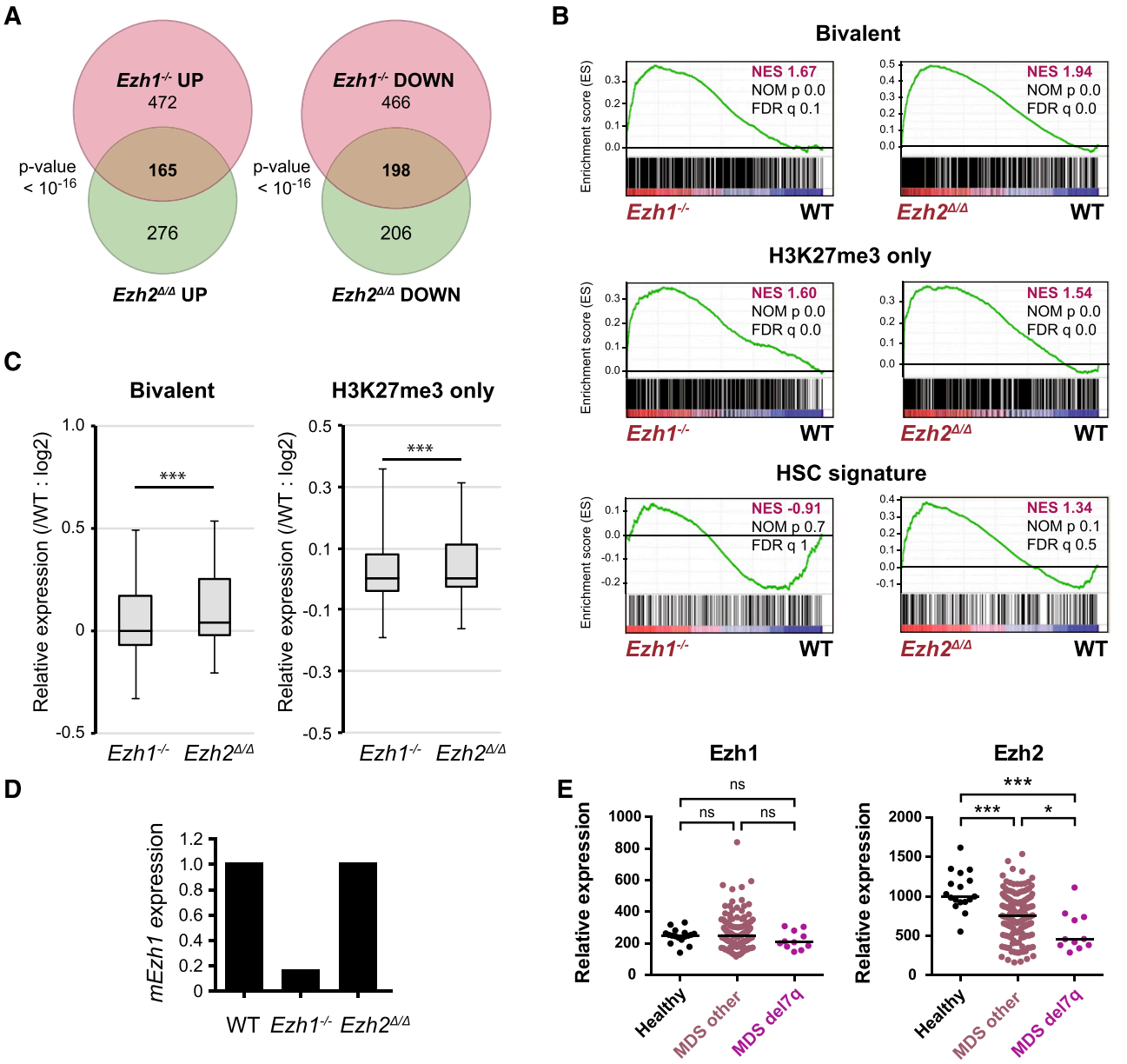

Figure 7. Gene expression profiles of *Ezh1*-deficient HSPCs. (A) Venn diagram showing the overlap between genes upregulated (at least twofold) and downregulated (at least twofold) in *Ezh1*$^{-/-}$ and *Ezh2*$^{\Delta/\Delta}$ LSK cells compared with WT LSK cells. RNA-sequence analysis was performed using LSK cells from WT, *Ezh1*$^{-/-}$, and *Ezh2*$^{\Delta/\Delta}$ mice at 1 month postinjection of tamoxifen. (B) GSEA plots demonstrating enrichment levels of indicated gene sets in *Ezh1*$^{-/-}$ and *Ezh2*$^{\Delta/\Delta}$ LSK cells compared with WT LSK cells. NES, NOM *P* value, and FDR are indicated. (C) Box-and-whisker plots showing the expression levels of H3K27me3-only genes and bivalent genes in *Ezh1*$^{-/-}$ and *Ezh2*$^{\Delta/\Delta}$ LSK cells relative to WT LSK cells. Boxes represent 25 to 75 percentile ranges. Vertical lines represent 10 to 90 percentile ranges. Horizontal bars represent median. ***$P < .001$ (Student *t* test.). (D) Graphic presentation of RNA-sequence data. RPKM of *Ezh1* in *Ezh1*$^{-/-}$ and *Ezh2*$^{\Delta/\Delta}$ LSK cells were shown relative to that of WT LSK cells. (E) Expression of *EZH1* and *EZH2* in CD34^{+} MDS cells. Relative expression of *EZH1* and *EZH2* in CD34^{+} cells from healthy controls, MDS patients, and MDS patients with 7q deletion. The data are presented as scatter diagrams with median values (bars). ***$P < .001$ (Student *t* test). The data from MDS patients were retrieved from published database.[38]

but support repositioning of EZH1 to EZH2 targets as suggested by ChIP-sequence data (Figure 4).

Discussion

In the present study, we demonstrated that the deletion of *Ezh2* caused heterogeneous hematopoietic malignancies including myelodysplastic disorders (MDS and MDS/MPN) and lymphoid leukemia in mice. These results support the tumor suppressive role of EZH2 in these diseases. In contrast, as we reported previously,[24,25] AML was not observed in our cohorts. This result confirmed the oncogenic role of EZH2 in AML, in which inactivating *EZH2* mutations are rare,[14,20,26,27] and the efficacy of EZH2 inhibitors was shown in preclinical studies.[10,39]

Corresponding to the recent finding that inactivating *EZH2* mutations were recurrently identified in patients with MDS and MDS/MPN,[13-20] Ezh2 loss alone in mice induced MDS and MDS/MPN after a long latency. In our previous study, we reported the development of MDS/MPN only.[24] However, we also observed the development of an MDS-like disease in this much larger cohort. These findings strongly support the role of inactivating *EZH2* mutations in the pathogenesis of myelodysplastic disorders. *EZH2* mutations are

acquired by the preceding HSC clones with founder mutations, such as *TET2* and *DNMT3A*, and splicing factor gene mutations,[16,40,41] which initiate and promote clonal hematopoiesis during aging.[40-42] Once additional mutations are acquired in founder clones or subclones, concurrent mutations are thought to cooperate in the progression of myelodysplastic disorders. We previously demonstrated cooperation between the *Tet2* hypomorph ($Tet2^{KD/KD}$) and Ezh2 loss in a mouse model of myelodysplastic disorders.[24] Although *TET2* mutations are more frequently detected in myelodysplastic disorders than *EZH2* mutations, the *Tet2* hypomorph did not cause obvious myelodysplasia in mice.[24] In contrast, Ezh2 loss induced myelodysplasia, particularly morphologic dysplasia, from the early time point in this study. Given that Asxl1 loss also leads to myelodysplasia through dysregulated H3K27me3 modification,[43] PRC2 insufficiencies may be closely associated with myelodysplasia.

In this study, we analyzed only homozygous inactivation of *Ezh2*. However, the majority of mutations in *EZH2* in human disease are heterozygous.[13-15] Of interest, we have previously evaluated the effect of heterozygous inactivation of *Ezh2* in *Tet2* gene trap mice ($Tet2^{KD/KD}$). The median survival was significantly shortened by heterozygous loss of *Ezh2* ($Tet2^{KD/KD}Ezh2^{\Delta/\Delta}$ mice [n = 20], $Tet2^{KD/KD}Ezh2^{\Delta/+}$mice [n = 14], and $Tet2^{KD/KD}Ezh2^{+/+}$ mice [n = 34] being 172 days, 243 days, and undetermined, respectively; $Tet2^{KD/KD}Ezh2^{\Delta/+}$mice vs $Tet2^{KD/KD}Ezh2^{+/+}$ mice, $P = .004$ by log-rank test). These data clearly suggest a haploinsufficient effect of *EZH2*.

PRC2 gene mutations, including *EZH2* mutations, are also frequently identified in adult T-ALL (25%)[34,44,45] as well as childhood early T-cell precursor (ETP) ALL (42%) and non-ETP ALL (12%).[46] We observed the development of T-cell receptor αβ (TCRαβ)-type T-ALL/lymphoma in the secondary transplantation of *Ezh2*-deficient hematopoietic cells. In contrast, TCRγδ-type T-ALL has been reported to develop much earlier in *Ezh2*-deficient mice.[44] These discrepancies may be due to the different designs of gene targeting and/or the different deleter mice used. It would be intriguing to ask why diverse malignancies, such as MDS, MDS/MPN, and T-ALL, developed in $Ezh2^{\Delta/\Delta}$ mice. Our expression profiling in this study did not provide any definite insight into this question. Only the epidermal growth factor signaling gene sets appeared to be significantly enriched in $CD8^+$ T-ALL cells (Figure 2F) but not in MDS or MDS/MPN LSK cells (data not shown). Further study is essential to understand the differential impacts of Ezh2 loss in hematologic malignancies.

Although inactivating *EZH2* mutations have yet to be identified in B-cell malignancies including CLL,[47] we often detected the expansion of B-1a B cells in *Ezh2*-deficient mice, some of which developed LPD or a CLL-like disease after a long latency. B-1 cells are innate-like lymphocytes that have important functions in immune defense, and are found at higher frequencies within the peritoneal and pleural cavities of mice.[48] Ezh2 loss has been shown to markedly affect the differentiation of B cells in the BM.[49] Consistent with these findings, we did not observe the development of any conventional B-cell malignancies in *Ezh2*-deficient mice. It is possible that the expansion of B-1 cells is secondary to the compromised differentiation of conventional B cells. However, Ezh2 may also be involved in the negative regulation of the differentiation of B-1 cells. The role of Dnmt3 in this regulation has been suggested by the recent finding that the loss of Dnmt3a alone or with Dnmt3b showed a strong propensity to induce B-1 CLL in FVB mice.[50]

In our gene expression analysis, bivalent genes appeared to be largely repressed in HSPCs over time in the absence of Ezh2. This could be partly due to replacement by DNA methylation following loss of H3K27me3 modification. However, ChIP-sequence data clearly showed that H3K27me3 levels at the promoters of PRC2 targets, particularly bivalent genes, significantly recovered over time in HSPCs. Recently, Ezh1 has been demonstrated to reposition to Ezh2 target genes upon depletion of Ezh2 in erythroid cells.[51] Correspondingly, H3K27me3 levels recovered not globally but in a locus-specific manner in this study. Given that the expression of Ezh1 does not change in the absence of Ezh2, repositioning of Ezh1 to Ezh2 target genes might be a promising mechanism underlying the compensatory function of Ezh1 for Ezh2.

In this study, an essential role for Ezh1 was confirmed by the finding that $Ezh1^{-/-}Ezh2^{\Delta/\Delta}$ HSCs could not support hematopoiesis. Ezh1 was found to be critical for transcriptional repression of $p15^{Ink4b}$, $p16^{Ink4a}$, and $p19^{Arf}$ in $Ezh2^{\Delta/\Delta}$ HSPCs. Indeed, conditional deletion of *Ezh1* in adult BM HSPCs has been reported to cause derepression of $p15^{Ink4b}$ and $p16^{Ink4a}$,[5] although straight knockout of *Ezh1* used in this study did not cause derepression of these genes. Given that the loss of Ezh1 has only a minimal impact on global H3K27me3 levels,[5] more comprehensive analysis is needed to understand Ezh1 function in HSPCs. Taken together, the results of the present study indicate that Ezh1 acts to maintain pathological stem cells under Ezh2 insufficiency and correspond well with the fact that no recurrent somatic mutations in *EZH1* have been identified in patients with hematologic malignancies. Our findings also suggest that patients with *EZH2* mutations would be more sensitive to EZH1 inhibition compared with patients without *EZH2* mutations. Although there is currently no EZH1-specific inhibitor, this possibility should be tested in the near future.

Accumulating evidence suggests that epigenetic abnormalities hold the key to the pathogenesis of hematologic malignancies.[52,53] The results of the present study provide a new mouse model for hematologic malignancies. Inactivating mutations targeting PRC2 components, such as *EED* and *SUZ12*, have recently been identified even in solid tumors.[54] Our mouse models may facilitate understanding of the tumor suppressor role of PRC2 not only in hematologic malignancies, but also in a broader range of cancers.

Acknowledgments

Ezh1 constitutive knockout mice were generated at the Research Institute of Molecular Pathology (Vienna, Austria) in 2000 by Dønal O'Carroll (Laboratory Thomas Jenuwein) with the help of Maria Sibilia (Laboratory Erwin Wagner) and will be reported elsewhere. $Ezh2^{fl/fl}$ mice were kindly provided by Haruhiko Koseki (RIKEN, Japan). The authors thank Ola Mohammed Kamel Rizq for critical review of the manuscript.

This work was supported in part by Grants-in-Aid for Scientific Research (#24249054) and Scientific Research on Innovative Areas "Stem Cell Aging and Disease" (#25115002) and "Cancer Stem Cell" (#25130702) from Ministry of Education, Culture, Sports, Science, and Technology (MEXT), Japan, and grants from the Naito Foundation, Uehara Memorial Foundation, and Takeda Science Foundation.

M.M.-K. is a research fellow supported by Japan Society for the Promotion of Science, MEXT, Japan.

Authorship

Contribution: M.M.-K. performed the experiments, analyzed results, made the figures, and actively wrote the manuscript; K.A., G.S., M.O., T.T., T.M., and C.W. assisted with the experiments; and A.I.

conceived of and directed the project, secured funding, and actively wrote the manuscript.

Conflict-of-interest disclosure: The authors declare no competing financial interests.

Correspondence: Atsushi Iwama, Department of Cellular and Molecular Medicine, Graduate School of Medicine, Chiba University, 1-8-1 Inohana, Chuo-ku, Chiba, 260-8670 Japan; e-mail: aiwama@faculty.chiba-u.jp.

References

1. Laugesen A, Helin K. Chromatin repressive complexes in stem cells, development, and cancer. *Cell Stem Cell.* 2014;14(6):735-751.
2. Comet I, Helin K. Revolution in the Polycomb hierarchy. *Nat Struct Mol Biol.* 2014;21(7):573-575.
3. Sauvageau M, Sauvageau G. Polycomb group proteins: multi-faceted regulators of somatic stem cells and cancer. *Cell Stem Cell.* 2010;7(3):299-313.
4. Oshima M, Iwama A. Epigenetics of hematopoietic stem cell aging and disease. *Int J Hematol.* 2014;100(4):326-334.
5. Hidalgo I, Herrera-Merchan A, Ligos JM, et al. Ezh1 is required for hematopoietic stem cell maintenance and prevents senescence-like cell cycle arrest. *Cell Stem Cell.* 2012;11(5):649-662.
6. Xie H, Xu J, Hsu JH, et al. Polycomb repressive complex 2 regulates normal hematopoietic stem cell function in a developmental-stage-specific manner. *Cell Stem Cell.* 2014;14(1):68-80.
7. Mochizuki-Kashio M, Mishima Y, Miyagi S, et al. Dependency on the polycomb gene Ezh2 distinguishes fetal from adult hematopoietic stem cells. *Blood.* 2011;118(25):6553-6561.
8. Tanaka S, Miyagi S, Sashida G, et al. Ezh2 augments leukemogenicity by reinforcing differentiation blockage in acute myeloid leukemia. *Blood.* 2012;120(5):1107-1117.
9. Neff T, Sinha AU, Kluk MJ, et al. Polycomb repressive complex 2 is required for MLL-AF9 leukemia. *Proc Natl Acad Sci USA.* 2012;109(13):5028-5033.
10. Xu B, On DM, Ma A, et al. Selective inhibition of EZH2 and EZH1 enzymatic activity by a small molecule suppresses MLL-rearranged leukemia. *Blood.* 2015;125(2):346-357.
11. Herrera-Merchan A, Arranz L, Ligos JM, de Molina A, Dominguez O, Gonzalez S. Ectopic expression of the histone methyltransferase Ezh2 in haematopoietic stem cells causes myeloproliferative disease. *Nat Commun.* 2012;3:623.
12. Morin RD, Johnson NA, Severson TM, et al. Somatic mutations altering EZH2 (Tyr641) in follicular and diffuse large B-cell lymphomas of germinal-center origin. *Nat Genet.* 2010;42(2):181-185.
13. Nikoloski G, Langemeijer SM, Kuiper RP, et al. Somatic mutations of the histone methyltransferase gene EZH2 in myelodysplastic syndromes. *Nat Genet.* 2010;42(8):665-667.
14. Ernst T, Chase AJ, Score J, et al. Inactivating mutations of the histone methyltransferase gene EZH2 in myeloid disorders. *Nat Genet.* 2010;42(8):722-726.
15. Bejar R, Stevenson K, Abdel-Wahab O, et al. Clinical effect of point mutations in myelodysplastic syndromes. *N Engl J Med.* 2011;364(26):2496-2506.
16. Papaemmanuil E, Gerstung M, Malcovati L, et al; Chronic Myeloid Disorders Working Group of the International Cancer Genome Consortium. Clinical and biological implications of driver mutations in myelodysplastic syndromes. *Blood.* 2013;122(22):3616-3627.
17. Haferlach T, Nagata Y, Grossmann V, et al. Landscape of genetic lesions in 944 patients with myelodysplastic syndromes. *Leukemia.* 2014;28(2):241-247.
18. Khan SN, Jankowska AM, Mahfouz R, et al. Multiple mechanisms deregulate EZH2 and histone H3 lysine 27 epigenetic changes in myeloid malignancies. *Leukemia.* 2013;27(6):1301-1309.
19. Lund K, Adams PD, Copland M. EZH2 in normal and malignant hematopoiesis. *Leukemia.* 2014;28(1):44-49.
20. Shih AH, Abdel-Wahab O, Patel JP, Levine RL. The role of mutations in epigenetic regulators in myeloid malignancies. *Nat Rev Cancer.* 2012;12(9):599-612.
21. Honda H, Nagamachi A, Inaba T. -7/7q- syndrome in myeloid-lineage hematopoietic malignancies: attempts to understand this complex disease entity. *Oncogene.* 2015;34(19):2413-2425.
22. Abdel-Wahab O, Adli M, LaFave LM, et al. ASXL1 mutations promote myeloid transformation through loss of PRC2-mediated gene repression. *Cancer Cell.* 2012;22(2):180-193.
23. Abdel-Wahab O, Pardanani A, Patel J, et al. Concomitant analysis of EZH2 and ASXL1 mutations in myelofibrosis, chronic myelomonocytic leukemia and blast-phase myeloproliferative neoplasms. *Leukemia.* 2011;25(7):1200-1202.
24. Muto T, Sashida G, Oshima M, et al. Concurrent loss of *Ezh2* and *Tet2* cooperates in the pathogenesis of myelodysplastic disorders. *J Exp Med.* 2013;210(12):2627-2639.
25. Sashida G, Harada H, Matsui H, et al. Ezh2 loss promotes development of myelodysplastic syndrome but attenuates its predisposition to leukaemic transformation. *Nat Commun.* 2014;5:4177.
26. Walter MJ, Shen D, Ding L, et al. Clonal architecture of secondary acute myeloid leukemia. *N Engl J Med.* 2012;366(12):1090-1098.
27. Cancer Genome Atlas Research Network. Genomic and epigenomic landscapes of adult de novo acute myeloid leukemia. *N Engl J Med.* 2013;368(22):2059-2074.
28. Shen X, Liu Y, Hsu YJ, et al. EZH1 mediates methylation on histone H3 lysine 27 and complements EZH2 in maintaining stem cell identity and executing pluripotency. *Mol Cell.* 2008;32(4):491-502.
29. Hirabayashi Y, Suzki N, Tsuboi M, et al. Polycomb limits the neurogenic competence of neural precursor cells to promote astrogenic fate transition. *Neuron.* 2009;63(5):600-613.
30. Ezhkova E, Lien WH, Stokes N, Pasolli HA, Silva JM, Fuchs E. EZH1 and EZH2 cogovern histone H3K27 trimethylation and are essential for hair follicle homeostasis and wound repair. *Genes Dev.* 2011;25(5):485-498.
31. Bae WK, Kang K, Yu JH, et al. The methyltransferases enhancer of zeste homolog (EZH) 1 and EZH2 control hepatocyte homeostasis and regeneration. *FASEB J.* 2015;29(5):1653-1662.
32. Subramanian A, Tamayo P, Mootha VK, et al. Gene set enrichment analysis: a knowledge-based approach for interpreting genome-wide expression profiles. *Proc Natl Acad Sci USA.* 2005;102(43):15545-15550.
33. Sun D, Luo M, Jeong M, et al. Epigenomic profiling of young and aged HSCs reveals concerted changes during aging that reinforce self-renewal. *Cell Stem Cell.* 2014;14(5):673-688.
34. Ntziachristos P, Tsirigos A, Van Vlierberghe P, et al. Genetic inactivation of the polycomb repressive complex 2 in T cell acute lymphoblastic leukemia. *Nat Med.* 2012;18(2):298-301.
35. Park IK, Qian D, Kiel M, et al. Bmi-1 is required for maintenance of adult self-renewing haematopoietic stem cells. *Nature.* 2003;423(6937):302-305.
36. Oguro H, Iwama A, Morita Y, Kamijo T, van Lohuizen M, Nakauchi H. Differential impact of Ink4a and Arf on hematopoietic stem cells and their bone marrow microenvironment in Bmi1-deficient mice. *J Exp Med.* 2006;203(10):2247-2253.
37. Chambers SM, Shaw CA, Gatza C, Fisk CJ, Donehower LA, Goodell MA. Aging hematopoietic stem cells decline in function and exhibit epigenetic dysregulation. *PLoS Biol.* 2007;5(8):e201.
38. Pellagatti A, Cazzola M, Giagounidis A, et al. Deregulated gene expression pathways in myelodysplastic syndrome hematopoietic stem cells. *Leukemia.* 2010;24(4):756-764.
39. Xu B, Konze KD, Jin J, Wang GG. Targeting EZH2 and PRC2 dependence as novel anticancer therapy [published online ahead of print May 28, 2015]. *Exp Hematol.* doi:10.1016/j.exphem.2015.05.001.
40. Jaiswal S, Fontanillas P, Flannick J, et al. Age-related clonal hematopoiesis associated with adverse outcomes. *N Engl J Med.* 2014;371(26):2488-2498.
41. Genovese G, Kähler AK, Handsaker RE, et al. Clonal hematopoiesis and blood-cancer risk inferred from blood DNA sequence. *N Engl J Med.* 2014;371(26):2477-2487.
42. Xie M, Lu C, Wang J, et al. Age-related mutations associated with clonal hematopoietic expansion and malignancies. *Nat Med.* 2014;20(12):1472-1478.
43. Abdel-Wahab O, Gao J, Adli M, et al. Deletion of Asxl1 results in myelodysplasia and severe developmental defects in vivo. *J Exp Med.* 2013;210(12):2641-2659.
44. Simon C, Chagraoui J, Krosl J, et al. A key role for EZH2 and associated genes in mouse and human adult T-cell acute leukemia. *Genes Dev.* 2012;26(7):651-656.
45. Durinck K, Goossens S, Peirs S, et al. Novel biological insights in T-cell acute lymphoblastic leukemia [published online ahead of print June 26, 2015]. *Exp Hematol.* doi:10.1016/j.exphem.2015.05.017.
46. Zhang J, Ding L, Holmfeldt L, et al. The genetic basis of early T-cell precursor acute lymphoblastic leukaemia. *Nature.* 2012;481(7380):157-163.
47. Landau DA, Carter SL, Stojanov P, et al. Evolution and impact of subclonal mutations in chronic lymphocytic leukemia. *Cell.* 2013;152(4):714-726.

48. Baumgarth N. The double life of a B-1 cell: self-reactivity selects for protective effector functions. *Nat Rev Immunol.* 2011;11(1):34-46.

49. Su I-H, Basavaraj A, Krutchinsky AN, et al. Ezh2 controls B cell development through histone H3 methylation and Igh rearrangement. *Nat Immunol.* 2003;4(2):124-131.

50. Peters SL, Hlady RA, Opavska J, et al. Tumor suppressor functions of Dnmt3a and Dnmt3b in the prevention of malignant mouse lymphopoiesis. *Leukemia.* 2014;28(5):1138-1142.

51. Xu J, Shao Z, Li D, et al. Developmental control of polycomb subunit composition by GATA factors mediates a switch to non-canonical functions. *Mol Cell.* 2015;57(2):304-316.

52. Issa J-PJ. The myelodysplastic syndrome as a prototypical epigenetic disease. *Blood.* 2013; 121(19):3811-3817.

53. Eriksson A, Lennartsson A, Lehmann S. Epigenetic aberrations in acute myeloid leukemia: early key events during leukemogenesis [published online ahead of print June 25, 2015]. *Exp Hematol.* doi:10.1016/j.exphem.2015.05.009.

54. De Raedt T, Beert E, Pasmant E, et al. PRC2 loss amplifies Ras-driven transcription and confers sensitivity to BRD4-based therapies. *Nature.* 2014;514(7521):247-251.